Proton-Transport Catalysis: A Systematic Study of the Rearrangement of the Isoformyl Cation to the Formyl Cation

Andrew J. Chalk and Leo Radom*

Contribution from the Research School of Chemistry, Australian National University, Canberra, ACT 0200, Australia

Received April 3, 1997. Revised Manuscript Received June 4, 1997[⊗]

Abstract: High level ab initio calculations at the G2** level of theory have been used to examine the effect of interaction with a series of small neutral molecules (X = He, Ne, Ar, CO, HF, N_2, H_2O, and NH_3) on the barrier for rearrangement of the isoformyl cation (HOC^+) to the formyl cation (HCO^+). Interaction with species (He, Ne, and Ar) whose proton affinities are *less than* that of CO at oxygen leads to a reduction in the barrier from the value (147 kJ mol^{-1}) in the isolated system, but the barrier remains positive. Interaction with molecules (HF and N_2) whose proton affinities lie *between* the proton affinities of CO at O and at C leads to the barrier becoming negative, thus allowing proton migration to take place without an overall barrier. Finally, interaction with molecules (H_2O and NH_3) whose proton affinities are *greater than* that of CO at C leads to a further lowering of the barrier; however, proton transfer to X rather than proton migration from O to C becomes energetically preferred. The most effective proton-transport catalysts for the rearrangement of HOC^+ to HCO^+ are thus molecules whose proton affinities lie between those of CO at O and at C.

Introduction

The isoformyl cation (HOC^+) is well-known from both experimental and theoretical studies to be much less stable than its isomer, the formyl cation (HCO^+), the energy difference being about 160 kJ mol^{-1}.[1−5] However, there is a significant barrier, of about 150 kJ mol^{-1}, separating the two isomers,[1,2] which ensures that both HCO^+ and HOC^+ can be observed as isolated species in the gas phase.[3−8] For example, the microwave spectra of both species have been recorded.[6,7] In addition, we note that both the formyl cation and the isoformyl cation are firmly established interstellar species.[9,10]

The barrier for the rearrangement of HOC^+ to HCO^+ has been found to be markedly reduced or even eliminated as a result of interaction with an external molecule.[1,5,8] More generally, the phenomenon of catalysis of proton migration by a small neutral molecule has been described by Bohme as proton-transport catalysis.[11] There have been a number of isolated examples of proton-transport catalysis reported in the literature.[11,12] However, the only systematic examination that we are aware of to date has been a very recent study of the catalysis of the interconversion of distonic radical cations and their conventional isomers.[13] Theory is ideally placed to carry out a systematic investigation of proton-transport catalysis. In this paper, we present the results of a systematic theoretical study for the prototypical example of the rearrangement of the isoformyl cation to the formyl cation. Results are reported for the rearrangement of the isolated isoformyl cation to the formyl cation as well as rearrangements catalyzed by a selection of small neutral molecules X (X = He, Ne, Ar, CO, HF, N_2, H_2O, and NH_3).

Methods and Results

Standard ab initio molecular orbital calculations[14] were carried out with the GAUSSIAN 94[15] and MOLPRO[16] programs with a modifica-

[⊗] Abstract published in *Advance ACS Abstracts,* July 15, 1997.

(1) Nobes, R. H.; Radom, L. *Chem. Phys.* **1981**, *60*, 1.

(2) See, for example: (a) Del Bene, J. E.; Frisch, M. J.; Raghavachari, K.; Pople, J. A. *J. Phys. Chem.* **1982**, *86*, 1529. (b) Dixon, D. A.; Komornicki, A.; Kraemer, W. P. *J. Chem. Phys.* **1984**, *81*, 3603. (c) DeFrees, D. J.; McLean, A. D. *J. Comp. Chem.* **1986**, *7*, 321. (d) Ma, N. L.; Smith, B. J.; Pople, J. A.; Radom, L. *J. Am. Chem. Soc.* **1991**, *113*, 7903. (e) Ma, N. L.; Smith, B. J.; Radom, L. *Chem. Phys. Lett.* **1992**, *197*, 573. (f) Yamaguchi, Y.; Richards, C. A.; Schaefer, H. F. *J. Chem. Phys.* **1995**, *101*, 8945.

(3) Harland, P. W.; Kim, N. D.; Petrie, S. A. H. *Aust. J. Chem.* **1989**, *42*, 9.

(4) Lias, S. G.; Bartmess, J. E.; Liebman, J. F.; Holmes, J. L.; Levin, R. D.; Mallard, W. G. *J. Phys. Chem. Ref. Data Suppl.* **1988**, *17*.

(5) Freeman, C. G.; Knight, J. S.; Love, J. G.; McEwan, M. J. *Int. J. Mass Spectrom. Ion Processes* **1987**, *80*, 255.

(6) Woods, R. C.; Saykally, R. J.; Anderson, T. G.; Dixon, T. A.; Szanto, P. G. *J. Chem. Phys.* **1981**, *75*, 4256.

(7) Gudeman, C. S.; Woods, R. C. *Phys. Rev. Lett.* **1982**, *48*, 1344.

(8) Wagner-Redeker, W.; Kemper, P. R.; Jarrold, M. F.; Bowers, M. T. *J. Chem. Phys.* **1985**, *83*, 1121.

(9) (a) Woods, R. C.; Gudeman, C. S.; Dickman, R. L.; Goldmsith, P. F.; Harguenin, G. R.; Irvine, W. M; Hjalmarson, Å.; Nyman L. Å.; Olofsson, H. *Astrophys. J.* **1983**, *270*, 583. (b) Ziurys, L. M.; Apponi, A. J. *Astrophys. J.* **1995**, *455*, L73.

(10) Buhl, D.; Snyder, L. E. *Nature* **1970**, *228*, 267.

(11) Bohme, D. K. *Int. J. Mass Spectrom. Ion Processes* **1992**, *115*, 95.

(12) See, for example: (a) Ferguson, E. E. *Chem. Phys. Lett.* **1989**, *156*, 319. (b) Petrie, S.; Freeman, C. G.; Meot-Ner, M.; McEwan, M. J.; Ferguson, E. E. *J. Am. Chem. Soc.* **1990**, *112*, 7121. (c) Bosch, E.; Lluch, J. M.; Bertran, J. *J. Am. Chem. Soc.* **1990**, *112*, 3868. (d) Petrie, S.; Freeman, C. G.; Meot-Ner, M.; McEwan, M. J.; Ferguson, E. E. *J. Am. Chem. Soc.* **1990**, *112*, 7121. (e) Fox, A.; Bohme, D. K. *Chem. Phys. Lett.* **1991**, *187*, 541. (f) Audier, H. E.; Millet, A.; Leblanc, D.; Morton, T. H. *J. Am. Chem. Soc.* **1992**, *114*, 2020. (g) Ruttink, P. J. A.; Burgers, P. C. *Org. Mass Spectrom.* **1993**, *28*, 1087. (h) Mourgues, P.; Audier, H. E.; Leblanc, D.; Hammerum, S. *Org. Mass. Spectrom.* **1993**, *28*, 1098. (i) Becker, H.; Schröder, D.; Zummack, W.; Schwarz, H. *J. Am. Chem. Soc.* **1994**, *116*, 1096. (j) Audier, H. E.; Leblanc, D.; Mourgues, P.; McMahon, T. B.; Hammerum, S. *J. Chem. Soc., Chem. Commun.* **1994**, 2329. (k) Chou, P. K.; Smith, R. L.; Chyall, L. J.; Kenttämaa, H. I. *J. Am. Chem. Soc.* **1995**, *117*, 4374. (l) Gauld, J. W.; Audier, H.; Fossey, J.; Radom, L. *J. Am. Chem. Soc.* **1996**, *118*, 6299.

(13) Gauld, J. W.; Radom, L. Submitted for publication.

(14) Hehre, W. J.; Radom, L.; Schleyer, P. v. R.; Pople, J. A. *Ab Initio Molecular Orbital Theory*; Wiley: New York, 1986.

(15) Frisch, M. J.; Trucks, G. W.; Schlegel, H. B.; Gill, P. M. W.; Johnson, B. G.; Robb, M. A.; Cheeseman, J. R.; Keith, T. A.; Petersson, G. A.; Montgomery, J. A.; Raghavachari, K.; Al-Laham, M. A.; Zakrzewski, V. G.; Ortiz, J. V.; Foresman, J. B.; Cioslowski, J.; Stefanov, B. B.; Nanayakkara, A.; Challacombe, M.; Peng, C. Y.; Ayala, P. Y.; Chen, W.; Wong, M. W.; Andres, J. L.; Replogle, E. S.; Gomperts, R.; Martin, R. L.; Fox, D. J.; Binkley, J. S.; Defrees, D. J.; Baker, J.; Stewart, J. J. P.; Head-Gordon, M.; Gonzalez, C.; Pople, J. A. GAUSSIAN 94, Revision D.1; Gaussian Inc.; Pittsburgh, PA, 1995.

S0002-7863(97)01055-X CCC: $14.00 © 1997 American Chemical Society

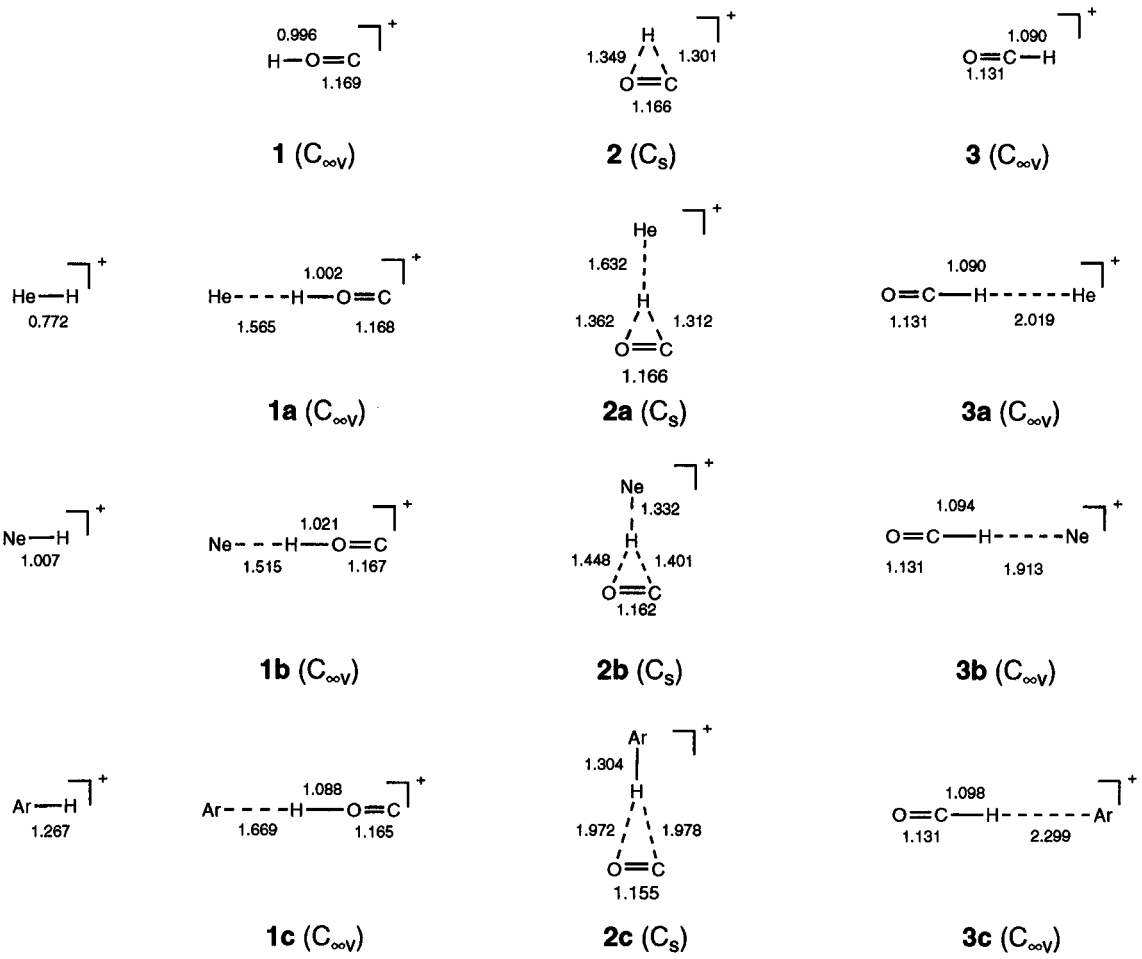

Figure 1. Selected MP2/6-31G(d,p) geometrical parameters for the isolated $[CHO]^+$ structures and for the $[X\cdots CHO]^+$ structures with X = He, Ne and Ar. Bond lengths in Å, bond angles in deg.

tion of the G2 level of theory.[17] G2 theory was introduced by Pople and co-workers with the aim of predicting thermochemical data to so-called chemical accuracy, roughly 10 kJ mol^{-1}. It corresponds effectively to calculations at the QCISD(T)/6-311+G(3df,2p) level on MP2/6-31G(d) optimized structures together with a zero-point vibrational energy (ZPVE) correction calculated at the (scaled) HF/6-31G(d) level and a so-called higher level correction. We have used a slight modification of G2 theory in the present work. Because we are dealing with proton-transfer reactions, we deemed it advisable to include polarization functions on hydrogen in the geometry optimizations (MP2/6-31G(d,p) instead of MP2/6-31G(d)). In addition, we have included polarization functions on hydrogen in the ZPVE calculations and carried these out at the MP2 level because several of the species under investigation are found to have different qualitative shapes at the HF and MP2 levels. Thus we have calculated the ZPVEs with MP2/6-31G(d,p) scaled by 0.9370[18] rather than HF/6-31G(d) scaled by 0.8929. We term this level of theory G2**. All electrons are correlated in the geometry optimizations and frequency calculations (i.e. MP2(full)). Calculated G2** total energies are listed in Table S1 of the Supporting Information. Selected geometrical features are displayed in Figures 1−3, while complete geometries are presented in the form of GAUSSIAN archive files in Table S2.

Discussion

The Isolated Isoformyl Cation−Formyl Cation Rearrangement. The potential energy profile for the rearrangement of the isolated isoformyl cation (**1**) to the formyl cation (**3**) via transition structure **2** is included in Figure 4. At the G2** level, the barrier is 147 kJ mol^{-1} and the exothermicity is 158 kJ mol^{-1}, consistent with previous results.[1−5]

Interaction with Helium. The smallest perturbation to the potential energy profile is provided by interaction with a helium atom, also included in Figure 4. Helium interacts weakly (by 7 kJ mol^{-1}) with HOC^+, to form the complex **1a**, it interacts a little more strongly (by 9 kJ mol^{-1}) with the transition structure **2** to give the transition structure **2a**, and it interacts weakly (by 2 kJ mol^{-1}) with HCO^+ to give the product complex **3a**. We note that this ordering of interaction energies, i.e., interaction of X with the transition structure > interaction of X with HOC^+ > interaction of X with HCO^+, is observed for all X. It is readily rationalizable in that the strongest interaction should occur with the weakest bond (as in the transition structure) and the weakest interaction with the strongest bond (as in HCO^+).

The barrier to rearrangement calculated relative to the separated reactants decreases slightly from 147 kJ mol^{-1} to 138 kJ mol^{-1}. This barrier lowering can be regarded as arising because interaction with helium weakens the H−O bond of HOC^+, thus making proton migration easier. Indeed, the bonds to the migrating proton are seen to be slightly longer in **1a** and **2a** compared with **1** and **2**, respectively (Figure 1).

Proton Affinities of X. Given this mechanism for barrier lowering, we might expect some correlation between the extent of barrier lowering and the proton affinity of the neutral molecule X: as the proton affinity of X is increased, the complex of X with HOC^+ will become stronger, the degree of bond weakening in the H−O bond of HOC^+ will be greater,

(16) MOLPRO is a package of *ab initio* programs written by H. J. Werner and P. J. Knowles with contributions from J. Almlöf, R. D. Amos, M. J. O. Deegan, S. T. Elbert, C. Hampel, W. Meyer, K. Peterson, R. Pitzer, A. J. Stone, P. R. Taylor, and R. Lindh.

(17) Curtiss, L. A.; Raghavachari, K.; Trucks, G. W.; Pople, J. A. *J. Chem. Phys.* **1991**, *94*, 7221.

(18) Scott, A. P.; Radom, L. *J. Phys. Chem.* **1996**, *100*, 16502.

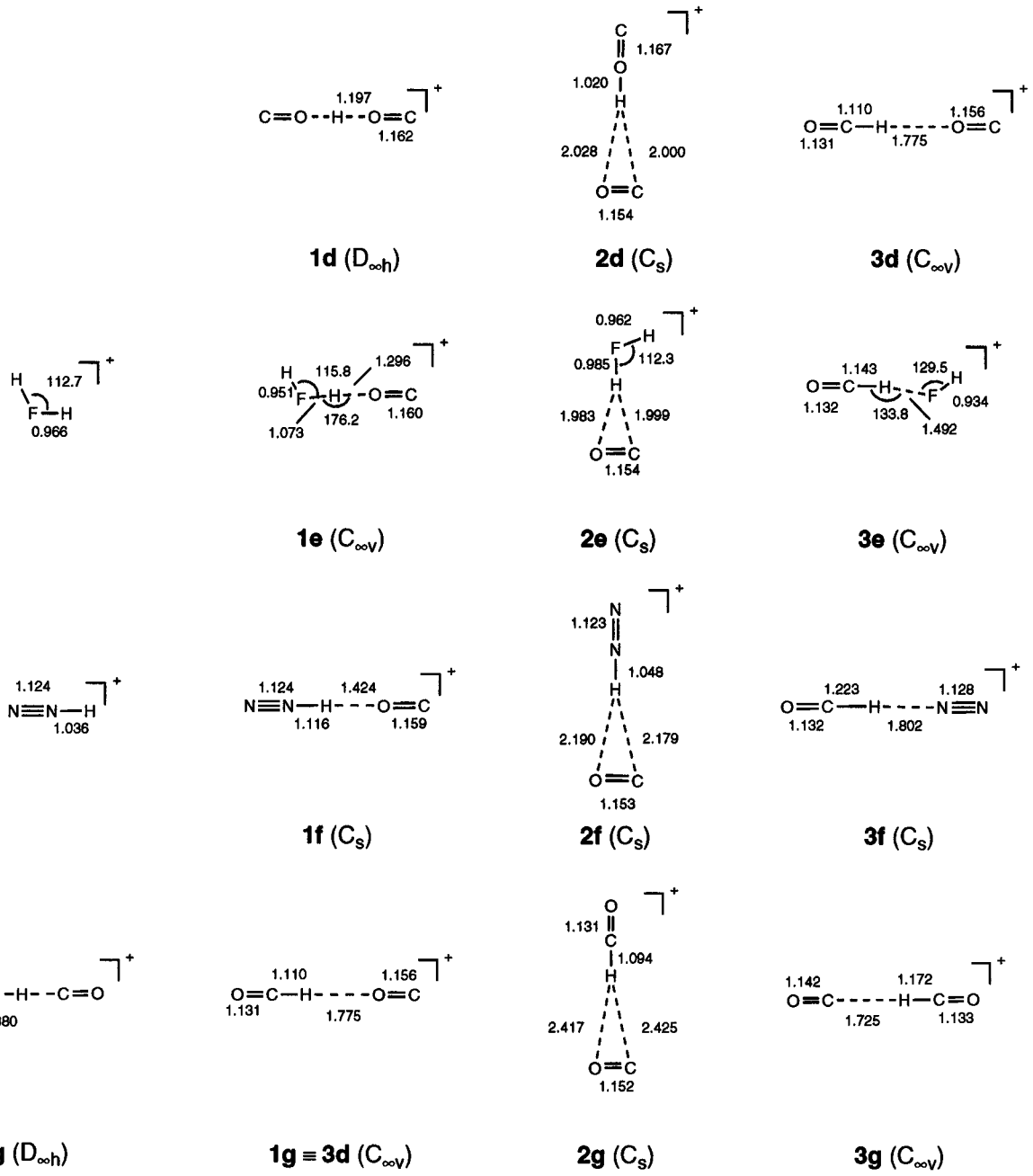

Figure 2. Selected MP2/6-31G(d,p) geometrical parameters for the $[X\cdots CHO]^+$ structures with X = CO*, HF, N_2, and *CO. Bond lengths in Å, bond angles in deg.

the proton migration will become easier, and hence the barrier will be lower.

The G2 level of theory has been found[19] to be very successful at predicting proton affinities, and this success would be expected to carry over smoothly to G2**. Comparison of calculated G2** proton affinities for the molecules X with experimental values[4,5] at 298 K (Table 1) shows that there is indeed good agreement between theory and experiment.[20]

Interaction with Neon and Argon. The proton affinities of neon and argon are greater than that of helium but smaller than that of CO at O (denoted CO*) (Table 1). Accordingly, we find that the interactions of Ne and Ar with the H of HOC^+ are greater and the barriers to proton migration are smaller than for He (Figures 1 and 4). However, the barriers remain positive. The barrier decreases from 147 kJ mol^{-1} in the isolated rearrangement to 138 kJ mol^{-1} for He, 131 kJ mol^{-1} for Ne, and just 33 kJ mol^{-1} for Ar.

Interaction with Hydrogen Fluoride, Nitrogen, and Carbon Monoxide. Molecules with proton affinities greater than He, Ne, and Ar are exemplified by carbon monoxide protonating at oxygen (CO*), hydrogen fluoride, molecular nitrogen, and carbon monoxide protonating at carbon (denoted *CO) (Table 1, Figure 2). The potential energy profiles of Figure 5 show that in all these cases the transition structures for rearrangement have dropped below the energy of the reactants X + HOC^+, i.e., the barriers have become negative. So interaction with CO, HF, and N_2 will allow HOC^+ to rearrange to HCO^+ without an overall barrier. We note that the interaction energy in the TS (e.g., 216 kJ mol^{-1} for X = HF) is again greater than that in either the reactant complex (132 kJ mol^{-1} for X = HF) or product complex (66 kJ mol^{-1} for X = HF).

N_2 and HF have proton affinities that lie between those of CO at oxygen and CO at carbon. They are therefore ideally

(19) For a detailed study, see: Smith, B. J.; Radom, L. *J. Am. Chem. Soc.* **1993**, *115*, 4885.

(20) The mean absolute deviation between theory and experiment is 4 kJ mol^{-1}, with a largest deviation of 11 kJ mol^{-1}.

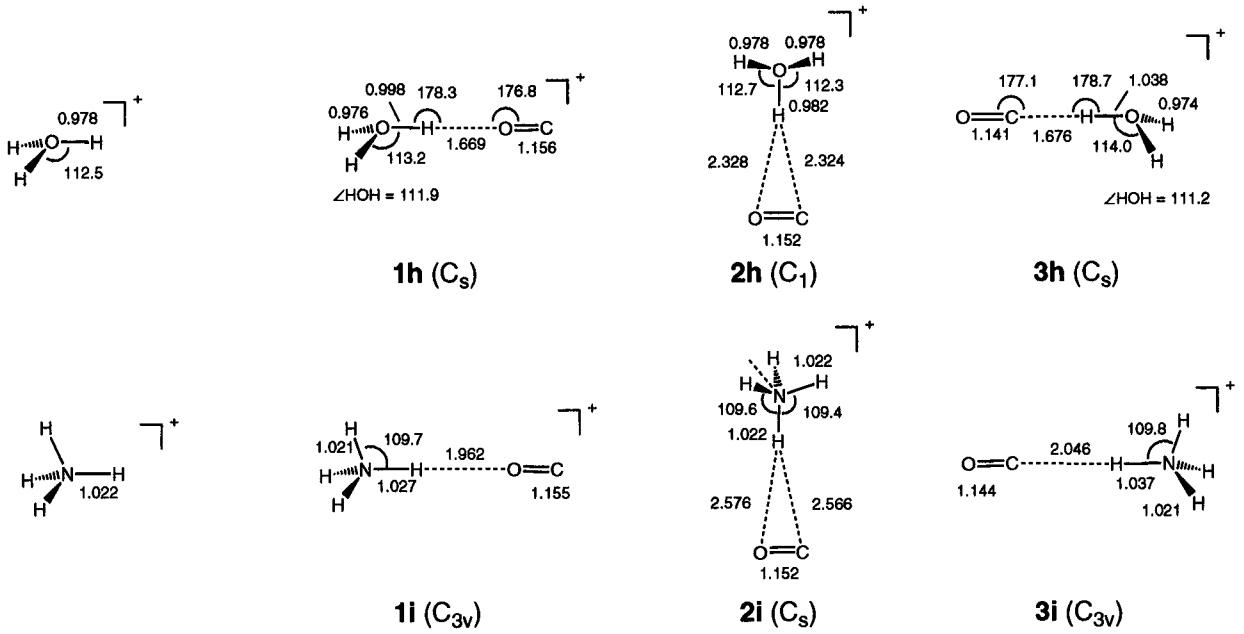

Figure 3. Selected MP2/6-31G(d,p) geometrical parameters for the $[X\cdots CHO]^+$ structures with X = H_2O and NH_3. Bond lengths in Å, bond angles in deg.

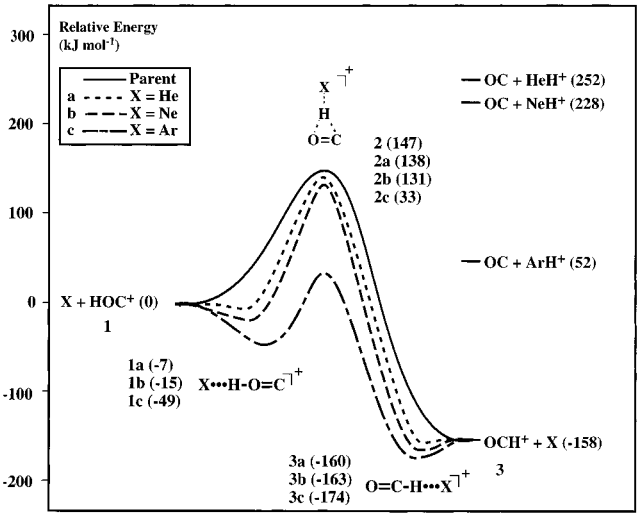

Figure 4. Schematic energy profile (G2**, 0 K) showing the uncatalyzed (parent) and catalyzed (X = He, Ne, and Ar) isomerization of the isoformyl cation to the formyl cation.

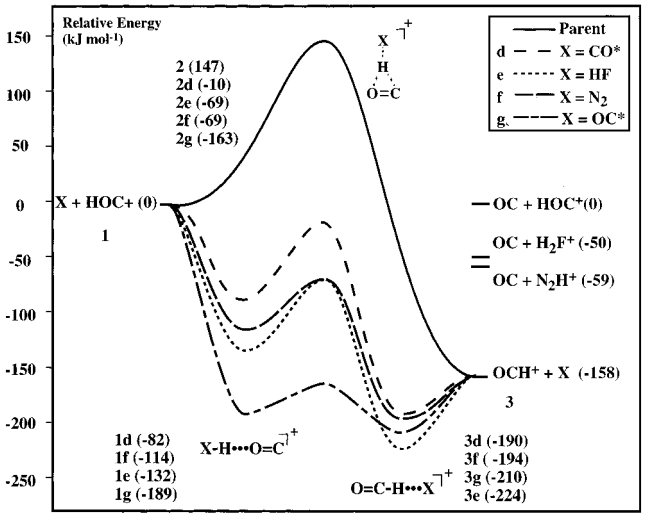

Figure 5. Schematic energy profile (G2**, 0 K) showing the uncatalyzed (parent) and catalyzed (X = CO*, HF, N_2, and *CO) isomerization of the isoformyl cation to the formyl cation.

Table 1. Calculated and Experimental Proton Affinities (kJ mol^{-1})[a]

	QCISD[b] 0 K	MP2[c] 0 K	G2** 0 K	G2** 298 K	expt[d] 298 K
He		210.2	177.8	181.5	178
Ne		222.0	201.9	205.6	201
Ar		369.4	377.8	381.6	371
CO*	434.8	431.5	430.1	433.5	427[e]
HF	485.9	520.5	480.3	485.3	489.5
N_2		493.6	488.9	494.4	494.5
*CO	594.8	612.8	588.2	593.9	594
H_2O		719.2	682.3	688.3	697
NH_3		882.9	847.9	854.2	854

[a] All calculated values include a scaled MP2/6-31G(d,p) ZPVE correction. [b] 6-311+G(d,p) basis set. [c] 6-31G(d,p) basis set. [d] All experimental values were taken from ref 4 unless otherwise noted. [e] From ref 5.

placed to drag a proton from HOC^+ to X and then to re-deposit it at carbon to produce HCO^+.

In the case of *CO a subtle difference in the potential surface is observed. In contrast to all the other complexes, **3g** has a double-well potential for proton transfer between the two components of the complex. However, once ZPVE is included the transition structure for proton transfer (shown as **4g**) is predicted to be lower in energy than that of **3g**, indicating a very flat potential for this type of motion.

Interaction with Water and Ammonia. Interaction with molecules whose proton affinity is greater than that for CO at carbon is exemplified by interaction with water (Table 1; Figures 3 and 6). The TS for rearrangement **2h** moves to very low energies, the barrier becoming −258 kJ mol^{-1}. It might seem at first sight that this would lead to even better catalysis. However, a problem arises because the proton affinity of water is *too* great. The water molecule captures a proton from HOC^+ quite readily, yielding a complex that can be described as $[H_2OH\cdots OC]^+$. However, it does not want to return the proton to the carbon end of CO to give HCO^+. Instead, it is energetically profitable for the water to retain the proton and form CO + H_3O^+ at −252 kJ mol^{-1} rather than HCO^+ + water at −158 kJ mol^{-1}. We do not have successful catalysis of the rearrangement any more because *inter*molecular proton transfer

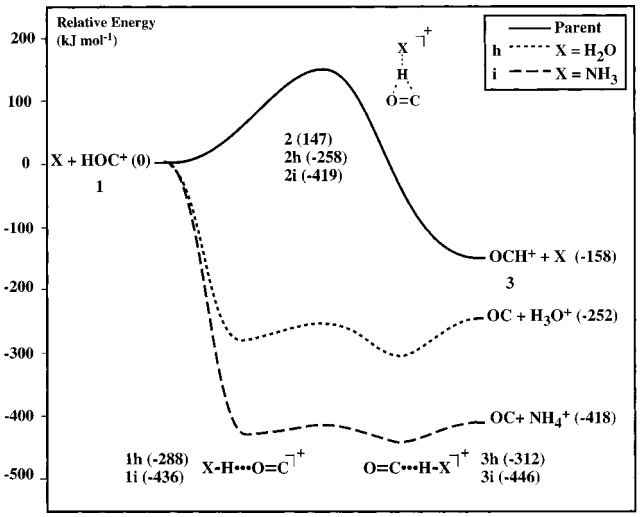

Figure 6. Schematic energy profile (G2**, 0 K) showing the uncatalyzed (parent) isomerization of the isoformyl cation to the formyl cation, and the formation of XH^+ in the presence of X = H_2O or NH_3.

Table 2. Relative Proton Affinities (ΔPA, kJ mol^{-1}),[a,b] H···O Bond Lengths in $[X{\cdots}H{\cdots}OC]^+$ Complexes (Å),[c] and Overall Reaction Barriers (kJ mol^{-1})[b,d]

X	Δ(PA)[a,b]	*r* (H···O)[c]	barrier[b,d]
		0.996	147
He	−252.3	1.002	138
Ne	−228.2	1.021	131
Ar	−52.3	1.088	33
CO*	0.0	1.197	−10
HF	50.2	1.296	−69
N_2	58.8	1.424	−69
*CO	158.1	1.775	−163
H_2O	252.2	1.669	−258
NH_3	417.8	1.962	−419

[a] Δ(PA) = PA(X) − PA(CO*). [b] G2** values at 0 K. [c] MP2/6-31G(d,p) optimized values. [d] Barrier relative to reactants X + HOC^+.

to produce H_3O^+ is preferred to the desired *intra*molecular proton migration to produce HCO^+.

A similar result is found for ammonia (Figures 3 and 6). The TS for rearrangement **2i** is now at −419 kJ mol^{-1} but the preferred product is NH_4^+ plus CO at −418 kJ mol^{-1} rather than NH_3 plus HCO^+ at −158 kJ mol^{-1} because the energy of the former is so much lower. Again, intermolecular proton transfer is energetically preferable to intramolecular proton migration.

General Comparisons. It is of interest to bring together some of the quantities relevant to the rearrangement process (Table 2). The first column of numbers lists the difference between the calculated proton affinity of X and that of CO at oxygen. The molecules are listed in order of increasing proton affinity. The next column gives the H···O distances in the initially formed complexes, $[X{\cdots}H{\cdots}OC]^+$. We can see, as expected, that the H···O distances increase relatively smoothly as the proton affinity of X increases. They start at 0.996 Å in HOC^+ itself and increase to 1.962 Å in the complex with NH_3 with its very large proton affinity. As this distance increases, we might expect the mobility of the proton to increase also. It is less tightly held. And indeed the barrier values show an excellent correlation, decreasing from 147 kJ mol^{-1} for the isolated rearrangement to −419 kJ mol^{-1} when X = NH_3.

The neutral molecules fall naturally into three groups. At the top, we have helium, neon, and argon. They have proton affinities smaller than that of CO at oxygen. They reduce the barriers from the value of 147 kJ mol^{-1} in the isolated system, but the barriers remain positive. Then we have HF and N_2 which have proton affinities lying between the values for CO at oxygen and CO at carbon. They are ideally placed for catalyzing the transfer of the proton from O to C. These reactions have no overall barrier. And finally we have water and ammonia which have proton affinities greater than that of CO at carbon. They can remove the proton from HOC^+ but they do not give it back. So they are not good catalysts.

Theoretical Considerations. It is of importance to attempt to assess the reliability of our G2** results in the present investigation. As noted early in this paper, G2 theory has been found to be very reliable for thermochemical predictions, and a similar level of performance would be expected to hold also for G2**. Nevertheless, it is desirable to examine the performance of G2** for the specific aspects of particular relevance to the present investigation.

Proton affinities are clearly of importance in the present study. We have already commented on the good agreement between G2** proton affinities and experimental values, as listed in Table 1. So this aspect is well catered for.

Next we consider the level of geometry optimization. The G2** calculations correspond to high level energy calculations, but these are carried out on geometries determined at the relatively modest MP2/6-31G(d,p) level of theory. MP2/6-31G(d,p) geometries would normally be expected to be quite adequate. However, the performance of MP2/6-31G(d,p) in the present study could depend in part on how well it describes the relative proton affinities of the various molecules X and CO because, for example, the geometry of the complex $[X{\cdots}H{\cdots}OC]^+$ depends very directly on the relative proton affinities of X and of CO at oxygen. A method that distorts these relativities would also distort the geometrical parameters from their true values.

The MP2/6-31G(d,p) proton affinities have been included in Table 1. We can see that the proton affinities at this level compare poorly with G2** values, showing deviations as large as 40 kJ mol^{-1}. In addition, these deviations vary considerably for different X, with the consequence that even the relative proton affinities compare poorly with G2** values. It is possible that the poor prediction of relative proton affinities by MP2/6-31G(d,p) may adversely affect the predicted structures, as noted above. To explore this possibility further, we have carried out additional calculations at the QCISD/6-311+G(d,p) level, initially obtaining proton affinities for CO at oxygen (CO*), hydrogen fluoride, and CO at carbon (*CO). As can be seen from Table 1, these proton affinities are in reasonable agreement with the G2** values, but more importantly, the deviations in the three cases are similar so that the relative proton affinities are in excellent agreement with G2**. We would therefore expect the QCISD/6-311+G(d,p) geometries for the X = hydrogen fluoride structures to provide an accurate benchmark against which to test the standard MP2/6-31G(d,p) structures.

Thus, in order to examine the possible effects of geometry on the calculated energies, the G2** procedure has been applied to QCISD/6-311+G(d,p) optimized geometries for X = HF. HF was chosen because it has the largest error in its proton affinity at the MP2/6-31G(d,p) level (Table 1), and we would therefore expect any geometry effects to be most pronounced in this system. The largest change observed is for the H···F bond in $OCH{\cdots}FH^+$ (**3e**), which increases from 1.492 (MP2/6-31G(d,p)) to 1.605 Å (QCISD/6-311+G(d,p)). However, because this is a weak bond, it does not have a large energetic effect. Indeed, the energies relative to the separated isoformyl cation and hydrogen fluoride calculated with QCISD/6-311+G(d,p) geometries for **1e** (−132.1 kJ mol^{-1}), **2e** (−70.3 kJ mol^{-1}) and **3e** (−227.5 kJ mol^{-1}) are reasonably close to the values calculated with the MP2/6-31G(d,p) geometries of −131.5, −69.3, and −224.2 kJ mol^{-1}, respectively. We conclude from

Table 3. Uncorrected and BSSE-Corrected Relative Energies (kJ mol^{-1})[a,b]

	$[X\cdots H\cdots OC]^+$			TS			$[OC\cdots H\cdots X]^+$		
X	uncorrected	$X + HOC^+$ [c]	$XH^+ + OC$[d]	uncorrected	$X + [HOC]^+$ [e]	$XH^+ + CO$[d]	uncorrected	$OCH^+ + X$[f]	$OC + HX^+$ [d]
He	−7	**−6**	−5	138	**139**	137	−160	**−159**	−161
Ne	−15	**−9**	−8	131	**138**	139	−163	**−160**	−157
Ar	−49	**−43**	−40	33	41	**36**	−174	**−172**	−169
CO*	−82	**−74**	**−74**	−10	−2	**−7**	−190	**−186**	−185
HF	−132	−122	**−124**	−69	−61	**−65**	−224	**−220**	−217
N_2	−114	−105	**−108**	−69	−61	**−66**	−194	**−189**	−188
OC*	−189	−184	**−188**	−163	−159	**−164**	−210	−206	**−207**
H_2O	−288	−280	**−283**	−258	−251	**−256**	−312	−303	**−308**
NH_3	−436	−431	**−435**	−419	−414	**−419**	−446	−440	**−445**

[a] All energies quoted are relative to separated X plus HOC^+. [b] Preferred BSSE partitioning shown in bold. [c] BSSE evaluated by partitioning into $X + HOC^+$. [d] BSSE evaluated by partitioning into $XH^+ + OC$. [e] BSSE evaluated by partitioning into $X + [HOC]^+$. [f] BSSE evaluated by partitioning into $OCH^+ + X$.

these results that the MP2/6−31G(d,p) level gives adequate geometries for our purposes.

Finally, in any ab initio study of weakly interacting systems it is important to investigate possible effects of basis set superposition error (BSSE). In the present work, we have estimated the magnitude of the BSSE for the complexes and transition structures by using the counterpoise method.[21] To apply this correction, it is necessary to divide the complexes and transition structures into two fragments. There are two obvious choices, namely X plus the appropriate $[CHO]^+$ isomer (or transition structure) or XH^+ plus CO. We have carried out calculations for both possible partitionings. Before discussing the results, we note that in the counterpoise method, it is necessary to calculate the energy of each fragment in its standard basis and in the full basis of the complex. For a composite method like G2**, this requires that each component single-point calculation that makes up the G2** energy be performed in the appropriate standard and full basis sets and the results combined in the usual way to give a G2** energy.

The uncorrected and BSSE-corrected energies of the complexes and transition structures, calculated relative to isolated X plus the isoformyl cation, are shown in Table 3. Our preferred BSSE partitioning, shown in bold in Table 3, corresponds to a division into the lower energy fragments since these are the fragments that the individual complexes and transition structures are most likely to resemble.[22] Interestingly, this partitioning also minimizes the BSSE correction. The effect of the BSSE correction in each case is to increase the relative energy, as expected. For our preferred partitioning, the average increases in energy relative to separated $X + HOC^+$ are 5, 3, and 3 kJ mol^{-1}, respectively, for $[X\cdots H\cdots OC]^+$, the TS, and $[OC\cdots H\cdots X]^+$, with maximum increases of 8, 7, and 5 kJ mol^{-1}. The BSSE correction thus raises fairly uniformly the part of the potential energy surface involving the complexes and transition structure relative to separated fragments, and it would therefore not affect our general conclusions.

(21) Boys, S. F.; Bernardi, F. *Mol. Phys.* **1970**, *19*, 553.
(22) Bouma, W. J.; Radom, L. *Chem. Phys. Lett.* **1979**, *64*, 216.

Concluding Remarks

Rearrangement of the isoformyl cation (HOC^+) to the formyl cation (HCO^+) is impeded by a substantial barrier of 147 kJ mol^{-1}. Interaction with a neutral molecule X leads to a significant lowering of the barrier. In the cases examined in the present study, if the proton affinity of X is less than that of CO at oxygen, the barrier is reduced but remains positive. If the proton affinity of X lies between the proton affinity of CO at O and at C, the barrier becomes negative. This is the ideal situation for effective catalysis. Finally, if the proton affinity of X lies above that of CO at carbon, the barrier is lowered further but the proton is preferentially transferred to X rather than migrating to C.

Acknowledgment. We gratefully acknowledge generous allocations of time on the Fujitsu VPP300 and SGI Power Challenge computers of the Australian National University Supercomputing Facility.

Supporting Information Available: Total G2** energies (Table S1) and GAUSSIAN 94 archive entries of the MP2/6-31G(d,p) optimized geometries (Table S2) (5 pages). See any current masthead for ordering and internet access instructions.

JA971055C